



Contents lists available at ScienceDirect

## Bioorganic &amp; Medicinal Chemistry Letters

journal homepage: [www.elsevier.com/locate/bmcl](http://www.elsevier.com/locate/bmcl)

## Hit to lead optimization of pyrazolo[1,5-*a*]pyrimidines as B-Raf kinase inhibitors

Ariamala Gopalsamy<sup>a,\*</sup>, Greg Ciszewski<sup>a</sup>, Mengxiao Shi<sup>a</sup>, Dan Berger<sup>a</sup>, Yongbo Hu<sup>a</sup>, Frederick Lee<sup>a</sup>, Larry Feldberg<sup>b</sup>, Eileen Frommer<sup>b</sup>, Steven Kim<sup>b</sup>, Karen Collins<sup>b</sup>, Donald Wojciechowicz<sup>b</sup>, Robert Mallon<sup>b</sup>

<sup>a</sup>Chemical and Screening Sciences, Wyeth Research, 401 N. Middletown Road, Pearl River, NY 10965, USA

<sup>b</sup>Discovery Oncology, Wyeth Research, 401 N. Middletown Road, Pearl River, NY 10965, USA

## ARTICLE INFO

## Article history:

Received 14 September 2009

Revised 15 October 2009

Accepted 19 October 2009

Available online 22 October 2009

## Keywords:

B-Raf inhibitor

Pyrazolo[1,5-*a*]pyrimidine

## ABSTRACT

Our continued effort towards optimization of the pyrazolo[1,5-*a*]pyrimidine scaffold as B-Raf kinase inhibitors is described. Structure guided design was utilized to introduce kinase hinge region interacting groups in the 2-position of the scaffold. This strategy led to the identification of lead compound **9** with enhanced enzyme and cellular potency, while maintaining good selectivity over a number of kinases.

© 2009 Elsevier Ltd. All rights reserved.

The RAS-RAF-MEK signal transduction pathway plays a key role in tumor biology.<sup>1</sup> A V600E mutation of the B-Raf isoform induces a constitutive activation of this kinase in the ERK pathway that increases cell proliferation and cell survival. Inhibitors of B-Raf could be used in the treatment of melanomas, colorectal cancer, and other Ras related human cancers.<sup>2</sup> A number of small molecule B-Raf inhibitors have been disclosed in the recent past including our high through-put screen<sup>3</sup> (HTS) effort that resulted in the identification of pyrazolo[1,5-*a*]pyrimidine-3-carboxylate **1** (Fig. 1).

As detailed in our previous Letter,<sup>4</sup> variations of the amide linker and the benzamide group substituents of compound **1** resulted in several sub-micromolar B-Raf inhibitors. Replacement of the ester group with amides was also tolerated, with increased activity for several amides bearing water solubilizing functionalities. However, from our proposed binding model of our HTS hit **1** with the B-Raf protein, no specific polar interaction was observed between the ester moiety and the protein. This observation prompted us to remove this metabolically labile moiety (microsomal stability—rat  $T_{1/2}$ : 8 min) and introduce groups in the 2-position of the pyrazolo[1,5-*a*]pyrimidine scaffold that could provide a potential hinge region interaction with the kinase. In this communication we detail our structure guided hit to lead optimization efforts on the pyrazolo[1,5-*a*]pyrimidine scaffold.

The analogs designed to obtain structure–activity relationships were synthesized by following the synthetic sequences shown in Schemes 1–3.<sup>5</sup> Pyridyl substituted aminopyrazole intermediate **4** was synthesized by condensation of the hydrazine with nitrile **3**,

which in turn was prepared from methyl isonicotinate **2**. Reaction of 3-nitroacetophenone **5** with *N,N*-dimethylformamidedimethylacetal followed by condensation with aminopyrazole **4** afforded pyrazolopyrimidine **7**. Reduction of the nitro group afforded the key intermediate aniline **8** which was further derivatized to the required amides by reacting with appropriate acid chlorides. Reaction of the common intermediate amine **8** with various isocyanates or triphosgene and appropriate amines generated urea analogs.

Synthetic analogs designed to identify optimal substituents on the 2-position of the pyrazolopyrimidine scaffold were generated starting from 3-substituted 5-aminopyrazoles **14** as shown in Scheme 2. The 3-trifluoromethylbenzamide moiety was introduced early on starting from 3-aminoacetophenone **15** which was converted to enamine **17** and condensed with aminopyrazole **14** to give *N*-(3-(2-morpholinopyrazolo[1,5-*a*]pyrimidin-7-yl)phenyl)-3-(trifluoromethyl)benzamide **18** (Scheme 2).

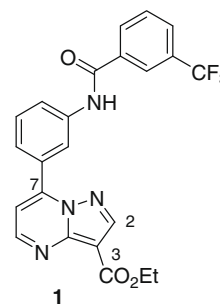
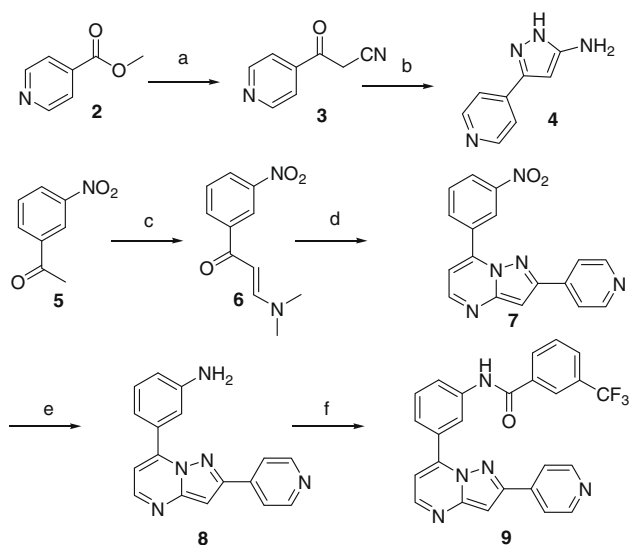


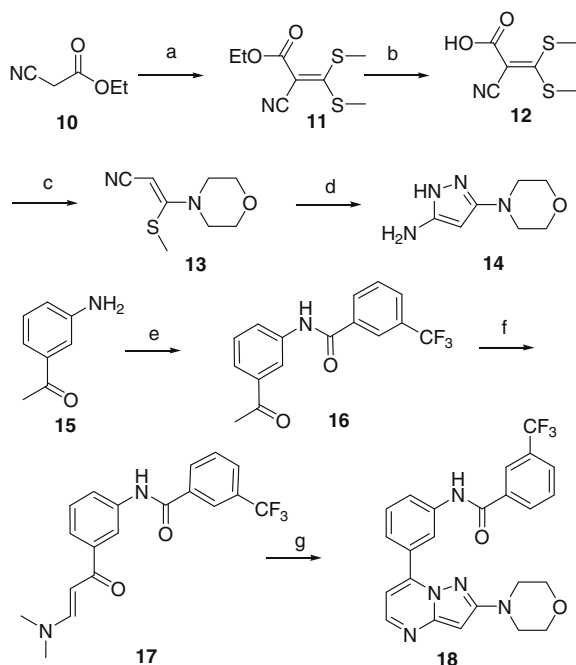
Figure 1. B-Raf inhibitor hit **1** identified from a high through-put screen.

\* Corresponding author.

E-mail address: [gopalsa@wyeth.com](mailto:gopalsa@wyeth.com) (A. Gopalsamy).



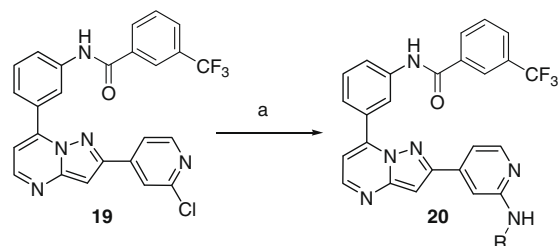
**Scheme 1.** Reagents and conditions: (a)  $\text{CH}_3\text{CN}$ , *t*-BuOK, toluene, reflux, 18 h, 52%; (b)  $\text{NH}_2\text{NH}_2$ , EtOH, reflux, 18 h, 65%; (c) DMF–DMA, reflux, 18 h, 79%; (d) **4**, HOAc, 80 °C, 18 h, 81%; (e) Fe, HOAc, 80 °C, 3 h, 72%; (f) pyridine, 3- $\text{CF}_3\text{PhCOCl}$ ,  $\text{CH}_2\text{Cl}_2$ , rt, 15 h, 71%.



**Scheme 2.** Reagents and conditions: (a)  $\text{K}_2\text{CO}_3$ ,  $\text{CS}_2$ , MeI, DMF, rt 8 h, 85%; (b) NaOH/THF, rt, 6 h, 30%; (c) morpholine,  $\text{Et}_3\text{N}$ , MeOH, rt, 8 h, 80%; (d) hydrazine, EtOH, reflux, 18 h, 100%; (e) 3- $\text{CF}_3\text{PhCOCl}$ , pyridine,  $\text{CH}_2\text{Cl}_2$ , 18 h, 100%; (f) DMF–DMA, 100 °C 18 h, 100%; (g) **14**, HOAc, 80 °C, 18 h, 80%.

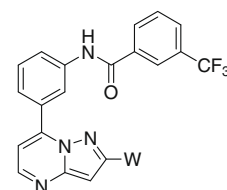
Analogs designed to introduce polar water solubilizing groups (compound **20**) were prepared starting from 2-chloropyridinyl pyrazolopyrimidine intermediate **19** under microwave condition using various amines as shown in Scheme 3.

Our SAR effort commenced with the placement of a variety of aromatic and heterocyclic rings in the 2-position of the pyrazolo-pyrimidine scaffold designed to reach out to the hinge region of the ATP binding pocket. While exploring this region, the 3-trifluoromethylbenzamide portion of the molecule was held constant. As seen from the representative examples in Table 1, evaluation of a number of substituted phenyl rings explored at the 2-position



**Scheme 3.** Reagents and conditions: (a)  $\text{RNH}_2$ , NMP or pyridine, microwave oven, 170 °C, 1–2 h.

**Table 1**  
SAR for 2-substituted pyrazolo[1,5-*a*]pyrimidine derivatives



Compds	W	B-Raf kinase $\text{IC}_{50}^a$ ( $\mu\text{M}$ )
<b>21</b>	3-Trifluoromethylphenyl	>10
<b>22</b>	4-Methoxyphenyl	>10
<b>23</b>	Thiophen-2-yl	>10
<b>24</b>	1 <i>H</i> -Imidazol-5-yl	1.6
<b>25</b>	1-Methyl-1 <i>H</i> -imidazol-5-yl	0.10
<b>9</b>	4-Pyridyl	0.032
<b>26</b>	3-Pyridyl	>10
<b>27</b>	Piperazin-1-yl	6.2
<b>28</b>	4-Methylpiperazin-1-yl	>10
<b>18</b>	Morpholino	0.099

<sup>a</sup> Values are means of two or more experiments.

led to a substantial loss in activity (compounds **21–22**). Of the heteroaromatic groups explored (compounds **23–26** and **9**), only the 4-pyridinyl analog **9** improved the enzyme potency significantly. The corresponding 3-pyridyl analog **26** was not favorable.

This observation was readily explained by our predicted binding pose for these analogs (Fig. 2), wherein a 4-pyridyl group is ideally positioned for the nitrogen atom to form hydrogen bond to Cys531 in the hinge region. This was further confirmed by the similar activity displayed by analogs **25** and **18** which can maintain

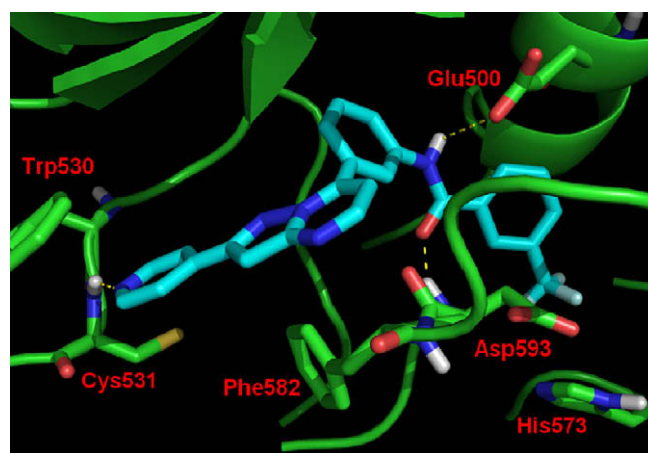
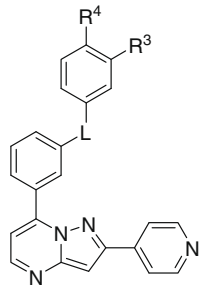


**Figure 2.** Predicted binding model of compound **9**. The pyridine nitrogen of the compound forms a hydrogen bond to the hinge region residue Cys531. The two hydrogen bonds from amide linker to Glu500 and Asp593 are maintained.

**Table 2**  
SAR for benzamide region of pyrazolo[1,5-*a*]pyrimidine derivatives



Compound	R <sup>3</sup>	R <sup>4</sup>	L	B-Raf IC <sub>50</sub> <sup>a</sup> (μM)
<b>29</b>	Cl	H	–NH–CO–	1.1
<b>30</b>	OCH <sub>3</sub>	H	–NH–CO–	4.0
<b>9</b>	CF <sub>3</sub>	H	–NH–CO–	0.032
<b>31</b>	Cl	Cl	–NH–CO–	0.66
<b>32</b>	CF <sub>3</sub>	Cl	–NH–CO–	0.060
<b>33</b>	CF <sub>3</sub>	H	–NH–CO–NH–	0.025
<b>34</b>	CF <sub>3</sub>	Cl	–NH–CO–NH–	0.040

<sup>a</sup> Values are means of two or more experiments.

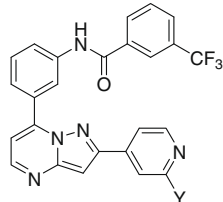
this hydrogen bond interaction with Cys531 due to the position of the ring nitrogen in the imidazole of **25** and the oxygen of the morpholine analog **18**. Piperazine analog **27**, which has a hydrogen bond donor instead of acceptor, was not tolerated. Analog **28**, which has an *N*-methylpiperazine moiety, was not favorable due to steric hindrance posed by the methyl group.

From our earlier optimization work, we have determined that the 3-trifluoromethyl substituted benzamide was preferred and was predicted to occupy a hydrophobic pocket created by Ile512, His513 and Ile571. The amide itself was involved in two hydrogen bonds to Glu500 and Asp593. In order to confirm that the 2-substituted pyrazolopyrimidines like **9** still retain these key interactions, we varied the substituents on the phenyl ring as shown by analogs **29–32** in Table 2. The SAR observed earlier for the HTS hit **1** was found to be reproducible for the 2-(4'-pyridyl)pyrazolo[1,5-*a*]pyrimidine scaffold. The flexibility shown by the linker to accommodate urea in the place of amide was found to be valid as shown by analogs **33–34**. A number of polar groups placed in the adjacent carbon atom of the pyridyl moiety were very well tolerated leading to a number of potent analogs as shown in Table 3. Docking studies indicated that these groups are ideally positioned to reach out to the solvent exposed region of the binding pocket.

Compound **9** was further profiled for its ability to inhibit proliferation in a variety of tumor cell lines. As seen from Table 4, the increased potency observed in the enzyme inhibition resulted in improvement in cellular growth inhibition. Compound **9**, in spite of invoking a hinge interaction in the ATP binding pocket of B-Raf enzyme, was found to be highly selective (IC<sub>50</sub>: >50 μM) against a number of kinases including CDK1, CDK2, PKBα, PKCα, PKCβ, IKKβ, JNK1, ERK2, P38α, MK2, PKA, ROCK1, CK1γ, Src, Fyn, Abl1, GCK, CHK1, RSK, PLK1, IGF1R, LCK, p70S6K, PI3Kα, m-TOR, Tpl2 and PDK1. Employing fluorescence spectroscopy techniques, compound **9** exhibited a single digit nanomolar K<sub>D</sub> from the changes in the endogenous tryptophan fluorescence of the enzyme upon inhibitor binding at the emission and excitation wavelengths of 465 nm and 295 nm, respectively. Compound **9** showed good permeability (PAMPA: 2.51 × 10<sup>-6</sup> m/s @ pH 7.4) and microsomal stability (rat T<sub>1/2</sub>: >30 min; nude mouse T<sub>1/2</sub>: 24 min).

In summary, the pyrazolopyrimidine scaffold identified as a B-Raf inhibitor from HTS has been modified to incorporate kinase

**Table 3**  
SAR for pyridine region modifications



Comps	Y	B-Raf kinase IC <sub>50</sub> <sup>a</sup> (μM)
<b>9</b>	H	0.032
<b>35</b>	–NHCH <sub>2</sub> CH <sub>2</sub> N(CH <sub>3</sub> ) <sub>2</sub>	0.053
<b>36</b>	–NHCH <sub>2</sub> CH <sub>2</sub> –N-morpholinyl	0.16
<b>37</b>	–NHCH <sub>2</sub> CH <sub>2</sub> CH <sub>2</sub> –N-morpholinyl	0.13
<b>38</b>	–NHCH <sub>2</sub> CH <sub>2</sub> –N-pyrrolidinyl	0.068
<b>39</b>	–NHCH <sub>2</sub> CH <sub>2</sub> CH <sub>2</sub> –N-pyrrolidinyl	0.11
<b>40</b>	–NHCH <sub>2</sub> CH <sub>2</sub> CH <sub>2</sub> –N-(2-oxo-pyrrolidinyl)	0.11
<b>41</b>	–NHCH <sub>2</sub> CH <sub>2</sub> CH <sub>2</sub> –N-(1 <i>H</i> -imidazolyl)	0.066
<b>42</b>	–NHCH <sub>2</sub> CH <sub>2</sub> –N-(4-hydroxy-piperidinyl)	0.066

<sup>a</sup> Values are means of two or more experiments.

**Table 4**  
Cell growth inhibition data

Tumor cell lines	Compound <b>1</b> IC <sub>50</sub> <sup>a</sup> (μM)	Compound <b>9</b> IC <sub>50</sub> <sup>a</sup> (μM)
A375	3.8	0.28
LoVo	3.87	0.4
HT29	7.0	0.35
CaCo-2	6.6	2.6
BXPC3	3.25	3.1
WM-266-4	6.2	3.5

<sup>a</sup> Values are means of two or more experiments.

hinge region interacting groups. This structure guided hit to lead optimization led to significant improvement in both enzyme and cellular activity while maintaining good selectivity over a number of kinases. Our continued effort in the area towards lead optimization will be communicated in the future.

## Acknowledgements

The authors thank Dr. John Ellingboe for his support of this work. We also thank Dr. Girija Krishnamurthy for K<sub>D</sub> determination and Wyeth Chemical Technologies group for analytical data.

## References and notes

- Garnett, M. J.; Marais, R. *Cancer Cell* **2004**, *6*, 313.
- Davies, H.; Bignell, G. R.; Cox, C.; Stephens, P.; Edkins, S.; Clegg, S.; Teague, J.; Woffendin, H.; Garnett, M. J.; Bottomley, W.; Davis, N.; Dicks, E.; Ewing, R.; Floyd, Y.; Gray, K.; Hall, S.; Hawes, R.; Hughes, J.; Kosmidou, V.; Menzies, A.; Mould, C.; Parker, A.; Stevens, C.; Watt, S.; Hooper, S.; Wilson, R.; Jayatilake, H.; Gusterson, B. A.; Cooper, C.; Shipley, J.; Hargrave, D.; Pritchard-Jones, K.; Maitland, N.; Chenevix-Trench, G.; Riggins, G. J.; Bigner, D. D.; Palmieri, G.; Cossu, A.; Flanagan, A.; Nicholson, A.; Ho, J. W. C.; Leung, S. Y.; Yuen, S. T.; Weber, B. L.; Seigler, H. F.; Darrow, T. L.; Paterson, H.; Marais, R.; Marshall, C. J.; Wooster, R.; Stratton, M. R.; Futreal, P. A. *Nature* **2002**, *417*, 949.
- Mallon, R.; Feldberg, L. R.; Kim, S. C.; Collins, K.; Wojciechowicz, D.; Hollander, L.; Kovacs, E. D.; Kohler, C. *Anal. Biochem.* **2001**, *294*, 48.
- Gopalsamy, A.; Ciszewski, G.; Hu, Y.; Lee, F.; Feldberg, L.; Frommer, E.; Kim, S.; Collins, K.; Wojciechowicz, D.; Mallon, R. *Bioorg. Med. Chem. Lett.* **2009**, *19*, 2735.
- For experimental details, see: Gopalsamy, A.; Ciszewski, G. M.; Shi, M.; Berger, D. M.; Torres, N.; Levin, J. I.; Powell, D. W. U.S. Pat. Appl. Publ., 2007; *Chem. Abstr.* **2007**, *147*, 386006.